14th International Conference on Information Fusion
Chicago, Illinois, USA, July 5-8, 2011

Particle filter for extracting target label information when targets move in close proximity

Ángel F. García-Fernández*, Mark R. Morelande†, Jesús Grajal*
*Dpto. Señales, Sistemas y Radiocomunicaciones, Universidad Politécnica de Madrid, Spain
†Melbourne Systems Laboratory, The University of Melbourne, Australia
Emails: agarcia@gmr.ssr.upm.es, mrmore@unimelb.edu.au, jesus@gmr.ssr.upm.es

***Abstract*—This paper addresses the problem of approximating the posterior probability density function of two targets after a crossing from the Bayesian perspective such that the information about target labels is not lost. To this end, we develop a particle filter that is able to maintain the inherent multimodality of the posterior after the targets have moved in close proximity. Having this approximation available, we are able to extract information about target labels even when the measurements do not provide information about target's identities. In addition, due to the structure of our particle filer, we are able to use an estimator that provides lower optimal subpattern assignment (OSPA) errors than usual estimators.**

***Index Terms*—Bayesian estimation, multitarget tracking, OSPA, particle filtering**

I. Introduction

There are two usual approaches to represent the multitarget state in multiple target tracking from the Bayesian perspective. One uses sets [1] and the other uses vectors [2], [3]. Set notation implies that targets are not labelled and, thus, one is not interested in knowing which target is which. All that matters is to estimate their states. Contrarily, in vector notation, the order implicit in the components of a vector implies that targets are labelled. Therefore, in this case, if the posterior probability density function (pdf) of the multitarget state is known, the information regarding target labels is included in the posterior, i.e., whether it is known which target is which and with what accuracy. The necessary and sufficient conditions the posterior for two targets must meet so that there is not any uncertainty regarding target labels are given in [4].

There are many cases of interest when the information about target labelling is useful. For example, let us assume there are two vehicles in an certain area. One is allied and the other is an enemy and they are being tracked by a sensor network equipped with seismic sensors. The vehicles have the same characteristics so the signal measured by the seismic sensors cannot tell them apart and their motions either. However, in the beginning, when the targets are far from each other, the association of targets and labels is obvious, i.e., we know which one is the friendly one and which one is the enemy. The problem arises when they get closer. In this case, it is difficult to indicate which target is which. However, as the posterior pdf contains all the available information, information about labelling is also included and can be extracted.

Particle filters (PFs) are a technique to approximate the posterior pdf when the system is nonlinear/non-Gaussian [5]. However, the necessary resampling stage used to overcome particle degeneracy implies that they are unable to reliably retain multiple modes of the posterior for extended periods [6], [7]. The problem is that, after a target crossing, the posterior pdf could be multimodal and it is in this multimodality where the information about target labelling lies. Therefore, a conventional PF is bound to lose this multimodality and, consequently, unable to provide information about target labels [6], [7]. In this paper, we propose a PF especially designed to provide information about target labelling maintaining this multimodality when two targets are present. Even though we address the two-target case, the methodology can be generalised for multiple targets in principle.

A further contribution of the paper is state estimation. When two targets are in close proximity for a long time, the minimum mean square error (MMSE) estimator always lies in the middle of positions of the targets so it is not useful [6], [7]. On the contrary, minimum mean OSPA estimator (MMOSPA) is expected to estimate the states of the targets properly as it does not label the estimated target states. However, it is very difficult to calculate and, to the authors knowledge, its implementation in a dynamic system has not been done yet [8]. The PF we propose readily enables us to use an estimator that roughly approximates the MMOSPA estimator under certain conditions. In general, this estimator gives rise to lower OSPA errors than the MMSE and maximum a posteriori (MAP) estimators without additional computational burden.

The remainder of the paper is organised as follows. In Section II, we introduce the problem in the Bayesian framework. In Section III, we indicate how information about target labelling is encoded in the posterior pdf and some of its properties. In Section IV, we explain the PF we use to extract the information about target labelling. We address target state estimation using the developed PF in Section V. Simulations are included in Section VI. Lastly, conclusions are drawn in Section VII.

II. Problem statement

We are going to analyse the problem of tracking two targets. The multitarget state vector at time k is represented by $\mathbf{X}^k = \left[\left(\mathbf{x}_1^k\right)^T, \left(\mathbf{x}_2^k\right)^T\right]^T \in \mathbb{R}^8$ where $\mathbf{x}_j^k$ is the state vector for target $j \in \{1, 2\}$ and the superscript T denotes transpose. The state vector for target j is $\mathbf{x}_j^k = \left[x_j^k, \dot{x}_j^k, y_j^k, \dot{y}_j^k\right]^T$ where $\mathbf{p}_j^k =$

$\left[x_j^k,\, y_j^k\right]^T$ is the position vector and $\mathbf{v}_j^k = \left[\dot{x}_j^k,\, \dot{y}_j^k\right]^T$ is the velocity vector.

The posterior pdf of the state given the sequence of measurements up to time k $\mathbf{z}^{1:k} = \left(\mathbf{z}^1,\, \mathbf{z}^2,\, ...,\, \mathbf{z}^k\right)$ can be calculated in two stages: prediction and update [9]. Assume that the posterior pdf at time k is available $\pi^k\left(\mathbf{X}^k\right)$. The pdf of the predicted state, prior pdf at time $k+1$, is calculated using the Chapman–Kolmogorov equation:

$$\varpi^{k+1}\left(\mathbf{X}^{k+1}\right) = \int f\left(\mathbf{X}^{k+1}\left|\mathbf{X}^k\right.\right)\pi^k\left(\mathbf{X}^k\right)\mathrm{d}\mathbf{X}^k \quad (1)$$

where $f\left(\mathbf{X}^{k+1}\left|\mathbf{X}^k\right.\right)$ is known and represents the dynamic equation for the targets. We also assume the targets move independently with similar dynamic models:

$$f\left(\mathbf{X}^{k+1}\left|\mathbf{X}^k\right.\right) = f_d\left(\mathbf{x}_1^{k+1}\left|\mathbf{x}_1^k\right.\right) f_d\left(\mathbf{x}_2^{k+1}\left|\mathbf{x}_2^k\right.\right) \quad (2)$$

where $f_d\left(\cdot\right)$ is the pdf that models the dynamics of one target and is the same for both targets.

The update equation is given by the Bayes' rule:

$$\pi^{k+1}\left(\mathbf{X}^{k+1}\right) \propto \ell\left(\mathbf{z}^{k+1}\left|\mathbf{X}^{k+1}\right.\right)\varpi^{k+1}\left(\mathbf{X}^{k+1}\right) \quad (3)$$

where $\propto$ denotes proportionality and $\ell\left(\mathbf{z}^{k+1}\left|\mathbf{X}^{k+1}\right.\right)$ is the likelihood.

In this paper, we assume that measurements do not provide any information about target identities. This implies that the likelihood is permutation invariant:

$$\ell\left(\mathbf{z}^{k+1}\left|\mathbf{X}^{k+1}\right.\right) = \ell\left(\mathbf{z}^{k+1}\left|\mathbf{\Pi}\mathbf{X}^{k+1}\right.\right) \quad (4)$$

where

$$\mathbf{\Pi} = \begin{pmatrix} 0 & 1 \\ 1 & 0 \end{pmatrix} \otimes \mathbf{I}_4 \quad (5)$$

where $\mathbf{I}_m$ is the $m \times m$ identity matrix, $\otimes$ is the Kronecker product and, consequently, $\mathbf{\Pi}$ is a matrix that permutes target 1 and 2 in the state vector:

$$\mathbf{\Pi}\mathbf{X}^k = \left[\left(\mathbf{x}_2^k\right)^T, \left(\mathbf{x}_1^k\right)^T\right]^T \quad (6)$$

Then, in principle, solving (1) and (3) recursively, we know everything about the targets as all the available information can be found in the posterior including that about target labelling.

III. Information about target labelling

In this section, we indicate how to get the information about target labelling considering we have available the posterior pdf given by (3). We provide a summary on some results found in [4] in subsections III-A, III-B and III-C. Moreover, we identify the regions that play an important role in target labelling in subsection III-D.

A. Permutation invariant pdf (with respect to $\mathbf{\Pi}$)

The posterior pdf is defined to be permutation invariant (with respect to $\mathbf{\Pi}$) if

$$\pi^k\left(\mathbf{X}^k\right) = \pi^k\left(\mathbf{\Pi}\mathbf{X}^k\right) \quad \forall\mathbf{X}^k \in \mathbb{R}^8 \quad (7)$$

In other words, we can interchange the state of both targets in the posterior pdf and the posterior is not altered. Therefore, it may be known where the two targets are, but each of the two target labels are equally probable, i.e., we do not know the correspondence between estimated positions and target labels. Then, in this case, we have lost all the information regarding the labels of the targets.

An interesting property that provides more insight on the problem can be noticed rewriting (7) as

$$\pi^k\left(\mathbf{X}^k\right) = \frac{1}{2}\left[\pi^k\left(\mathbf{X}^k\right) + \pi^k\left(\mathbf{\Pi}\mathbf{X}^k\right)\right] \quad (8)$$

The corresponding random finite set (RFS) density of the ordered posterior density, given by (3), is [1], [8]:

$$\pi^k\left(\left\{\mathbf{x}_1^k,\, \mathbf{x}_2^k\right\}\right) = \pi^k\left(\mathbf{X}^k\right) + \pi^k\left(\mathbf{\Pi}\mathbf{X}^k\right) \quad (9)$$

Therefore, comparing (8) and (9), it is clear that the RFS density and the ordered density are proportional when the ordered density is permutation invariant[1]. The reason for this is that the information of order (labelling) is lost when the posterior is permutation invariant. As a result, the posterior has exactly the same information as the posterior of a set.

B. Permutation strictly variant pdf (with respect to $\mathbf{\Pi}$)

The posterior pdf is defined to be permutation strictly variant (with respect to $\mathbf{\Pi}$) if

$$\pi^k\left(\mathbf{X}^k\right) \cdot \pi^k\left(\mathbf{\Pi}\mathbf{X}^k\right) = 0 \quad \forall\mathbf{X}^k \in \mathbb{R}^8 \quad (10)$$

This implies that for every possible state $\mathbf{X}^k$, such that $\pi^k\left(\mathbf{X}^k\right) > 0$, $\mathbf{\Pi}\mathbf{X}^k$ is not possible to occur taking into account all the available information given by the measurements plus the prior at time 0. Consequently, when the posterior pdf of two targets is strictly variant, there is no uncertainty at all regarding target labelling.

C. Unique decomposition of a pdf

When the posterior pdf is not either invariant or strictly variant, it is shown in [4] that it admits a unique decomposition

$$\pi^k\left(\mathbf{X}^k\right) = \alpha^k\pi_I^k\left(\mathbf{X}^k\right) + \left(1-\alpha^k\right)\pi_V^k\left(\mathbf{X}^k\right) \quad (11)$$

where $\pi_V^k\left(\mathbf{X}^k\right)$ is a permutation strictly variant pdf and $\pi_I^k\left(\mathbf{X}^k\right)$ is a permutation invariant pdf and

$$\alpha^k = \int \min\left[\pi^k\left(\mathbf{X}^k\right), \pi^k\left(\mathbf{\Pi}\mathbf{X}^k\right)\right]\mathrm{d}\mathbf{X}^k \quad (12)$$

$$\pi_I^k\left(\mathbf{X}^k\right) = \min\left[\pi^k\left(\mathbf{X}^k\right), \pi^k\left(\mathbf{\Pi}\mathbf{X}^k\right)\right]/\alpha^k \quad (13)$$

$$\pi_V^k\left(\mathbf{X}^k\right) = \left[\pi^k\left(\mathbf{X}^k\right) - \alpha^k\pi_I^k\left(\mathbf{X}^k\right)\right]/\left(1-\alpha^k\right) \quad (14)$$

Therefore, the parameter $\alpha^k \in [0,\, 1]$ indicates how invariant a posterior pdf is. If $\alpha^k = 1$, we have lost the target labels, if $\alpha^k = 0$ we perfectly know the labels of the targets and if $\alpha^k \in (0,\, 1)$, we are in an intermediate situation where the target labels can be confused.

[1]There is a proportionality constant because set integrals are defined differently than their vector counterparts.

D. Regions of interest of the unique decomposition

Here, we will develop an equivalent way to calculate the variant and invariant part of a pdf, given by (13) and (14). This new interpretation will allow us to build a PF that preserves multimodality with an easier notation in Section IV.

We define the region A^k as

$$A^k = \left\{\mathbf{X}^k \in \mathbb{R}^8 : \pi^k\left(\mathbf{X}^k\right) < \pi^k\left(\mathbf{\Pi}\mathbf{X}^k\right)\right\}$$

$$= \left\{\mathbf{X}^k \in \mathbb{R}^8 : \varpi^k\left(\mathbf{X}^k\right) < \varpi^k\left(\mathbf{\Pi}\mathbf{X}^k\right)\right\} \quad (15)$$

and its complement

$$\bar{A}^k = \left\{\mathbf{X}^k \in \mathbb{R}^8 : \mathbf{X}^k \notin A^k\right\} \quad (16)$$

where we have used (3) and (4). There are two important aspects that should be highlighted. The first one is that if the posterior is permutation invariant or permutation strictly variant, $A^k = \emptyset$ and $\bar{A}^k = \mathbb{R}^8$. The second one is that if $\alpha^k \in (0,1)$:

$$\mathbf{X}^k \in A^k \leftrightarrow \mathbf{\Pi}\mathbf{X}^k \in \bar{A}^k \quad (17)$$

According to the definitions (15) and (16), (13) and (14) can be written as

$$\pi_I^k\left(\mathbf{X}^k\right) = \left[\pi^k\left(\mathbf{X}^k\right)\chi_{A^k}\left(\mathbf{X}^k\right) + \pi^k\left(\mathbf{\Pi}\mathbf{X}^k\right)\chi_{\bar{A}^k}\left(\mathbf{X}^k\right)\right]/\alpha^k \quad (18)$$

$$\pi_V^k\left(\mathbf{X}^k\right) = \chi_{\bar{A}^k}\left(\mathbf{X}^k\right)\left[\pi^k\left(\mathbf{X}^k\right) - \pi^k\left(\mathbf{\Pi}\mathbf{X}^k\right)\right]/\left(1-\alpha^k\right) \quad (19)$$

and α^k is

$$\alpha^k = 2\int \pi^k\left(\mathbf{X}^k\right)\chi_{A^k}\left(\mathbf{X}^k\right)\mathrm{d}\mathbf{X}^k \quad (20)$$

and $\chi_{A^k}(\cdot)$ is the indicator function on the region A^k and we have assumed that $\alpha^k \in (0,1)$.Then, if we need to estimate α^k accurately, we should approximate the posterior pdf in regions A^k and $\bar{A}^k$ appropriately. The reason is due to (20) in which it is shown that α^k can be calculated as two times the integral of the posterior in region A^k.

IV. Particle filter implementation

Our objective is to approximate the posterior pdf such that we are able to calculate α^k for systems that are not necessarily linear and Gaussian. In this case, PFs are a technique to approximate the posterior [5]. However, they have an important shortcoming: if the posterior is multimodal, they cannot keep multimodality for a long time due to the necessary resampling stage [10]. From its definition, $\pi_I^k(\cdot)$ is permutation invariant with respect to $\mathbf{\Pi}$. Then, if there is a mode centred at $\mathbf{X}^k$, there will be another centred at $\mathbf{\Pi}\mathbf{X}^k$. Then, the permutation invariant part of the posterior pdf is multimodal and conventional PFs fail to estimate α^k properly as they can only approximate one mode for a long time [6], [7].

As we need to approximate the posterior accurately in regions A^k and $\bar{A}^k$, we can take into account that we know where the other mode is located if it exists, use (17) and approximate the posterior as

$$\pi^k\left(\mathbf{X}^k\right) \approx \sum_{i=1}^{N_{par}} w_i^k \delta\left(\mathbf{X}^k - \mathbf{X}_i^k\right) + u_i^k \delta\left(\mathbf{X}^k - \mathbf{\Pi}\mathbf{X}_i^k\right) \quad (21)$$

where N_{par} is the number of particles in the regions A^k and $\bar{A}^k$, $\delta(\cdot)$ is the Dirac delta, $\mathbf{X}_i^k$ is the multitarget state of particle i which belongs to $\bar{A}^k$ with weight w_i^k, $\mathbf{\Pi}\mathbf{X}_i^k$ is the "mirror" particle of $\mathbf{X}_i^k$ in A^k with weight u_i^k. The estimated value of α^k using (21) and (20) is:

$$\alpha^k \approx 2\sum_{i=1}^{N_{par}} u_i^k \quad (22)$$

The PF approximation of the posterior given by (21) can be seen as a PF that explores multimodality as we know that multimodality can exist because of the property of the permutation invariant part of the pdf. If the posterior is unimodal, which can only happen is the posterior is strictly variant, $u_i^k = 0$ for $i = 1, ..., N_{par}$.

In order to get a PF approximation of the posterior at time $k+1$ with the form (21) based on a PF approximation of the posterior at time k also with the form (21), there are two aspects that should be taken into account for any implementation regardless of the importance density we use. The first one is the approximation of A^{k+1} based on (21). The second one has to do with the fact that we always sample $\mathbf{X}_i^k$ and $\mathbf{\Pi}\mathbf{X}_i^k$. These aspects as well as our PF implementation are addressed in this section.

A. Approximation of the region A^{k+1}

Assuming the posterior at time k is represented by (21), using (1), the prior at time $k+1$ is

$$\varpi^{k+1}\left(\mathbf{X}^{k+1}\right) = \sum_{i=1}^{N_{par}} w_i^k f\left(\mathbf{X}^{k+1}\middle|\mathbf{X}_i^k\right) + u_i^k f\left(\mathbf{X}^{k+1}\middle|\mathbf{\Pi}\mathbf{X}_i^k\right) \quad (23)$$

Substituting (23) into (15), the region A^{k+1} becomes:

$$A^{k+1} = \left\{\mathbf{X}^{k+1} \in \mathbb{R}^8 : \right.$$

$$\sum_{i=1}^{N_{par}} w_i^k f\left(\mathbf{X}^{k+1}\middle|\mathbf{X}_i^k\right) + u_i^k f\left(\mathbf{X}^{k+1}\middle|\mathbf{\Pi}\mathbf{X}_i^k\right) <$$

$$\left.\sum_{i=1}^{N_{par}} w_i^k f\left(\mathbf{X}^{k+1}\middle|\mathbf{\Pi}\mathbf{X}_i^k\right) + u_i^k f\left(\mathbf{X}^{k+1}\middle|\mathbf{X}_i^k\right)\right\} \quad (24)$$

B. Exploration of the mirror mode

In the PF approximation of (21), we force the creation of the particles $\mathbf{\Pi}\mathbf{X}_i^k$ $i = 1, ..., N_{par}$ because we know that the posterior pdf in the area the symmetric particles lie could be high, especially after a target crossing, and that part of the posterior carries important information about the target labels. In this section, we explain the importance density we use to draw particles this way.

Let us assume we draw an intermediate sample from an importance density $\tilde{\mathbf{X}} \sim \upsilon(\cdot)$ and define the conditional pdf:

$$\upsilon_c\left(\mathbf{X}^k \middle| \tilde{\mathbf{X}}\right) = \frac{1}{2}\delta\left(\mathbf{X}^k - \tilde{\mathbf{X}}\right) + \frac{1}{2}\delta\left(\mathbf{X}^k - \mathbf{\Pi}\tilde{\mathbf{X}}\right) \quad (25)$$

The pdf $\upsilon_c\left(\cdot \middle| \tilde{\mathbf{X}}\right)$ is perfectly represented by the particles $\mathbf{X}_i^k = \tilde{\mathbf{X}}$ and $\mathbf{X}_{i+N_{par}}^k = \mathbf{\Pi}\tilde{\mathbf{X}}$. Therefore, the particles we use to represent the posterior can be thought to be drawn in the following way. Firstly, we draw $\tilde{\mathbf{X}} \sim \upsilon(\cdot)$ and then we assign the two samples that represent (25), $\mathbf{X}_i^k = \tilde{\mathbf{X}}$ and $\mathbf{X}_{i+N_{par}}^k = \mathbf{\Pi}\tilde{\mathbf{X}}$. The importance density $q(\cdot)$ we are using to obtain $\mathbf{X}_i^k$ and $\mathbf{X}_{i+N_{par}}^k$ can be calculated by integrating out $\tilde{\mathbf{X}}$ in the joint pdf of $\mathbf{X}^k$ and $\tilde{\mathbf{X}}$:

$$q\left(\mathbf{X}^k\right) = \int \upsilon_c\left(\mathbf{X}^k, \tilde{\mathbf{X}}\right) \mathrm{d}\tilde{\mathbf{X}} = \int \upsilon_c\left(\mathbf{X}^k \middle| \tilde{\mathbf{X}}\right) \upsilon\left(\tilde{\mathbf{X}}\right) \mathrm{d}\tilde{\mathbf{X}}$$

$$= \int \frac{1}{2}\left[\delta\left(\mathbf{X}^k - \tilde{\mathbf{X}}\right) + \delta\left(\mathbf{X}^k - \mathbf{\Pi}\tilde{\mathbf{X}}\right)\right] \upsilon\left(\tilde{\mathbf{X}}\right) \mathrm{d}\tilde{\mathbf{X}} \quad (26)$$

For any permutation matrix $\mathbf{\Pi}$, it holds that $\mathbf{\Pi}^{-1} = \mathbf{\Pi}^T$ and $|\det(\mathbf{\Pi})| = 1$ where $\det(\mathbf{\Pi})$ is the determinant of $\mathbf{\Pi}$ [11]. In addition, when there are only two targets $\mathbf{\Pi}^{-1} = \mathbf{\Pi}$. Therefore, we can write (26) as

$$q\left(\mathbf{X}^k\right) = \frac{1}{2}\left(\upsilon\left(\mathbf{X}^k\right) + \upsilon\left(\mathbf{\Pi}\mathbf{X}^k\right)\right) \quad (27)$$

C. Problems with conventional particle filters

According to the definition of α^{k+1}, $\alpha^{k+1} \in [0, 1]$ [4]. However, the conventional PFs based on sequential importance sampling or auxiliary sampling [9] can provide values of $\alpha^{k+1} > 1$ as explained in the following. Therefore, conventional PFs give rise to this undesirable situation.

Let us write the posterior, given by (3) and (23), as

$$\pi^{k+1}\left(\mathbf{X}^{k+1}, i\right) \propto \ell\left(\mathbf{z}^{k+1} \middle| \mathbf{X}^{k+1}\right) \cdot \varpi^{k+1}\left(\mathbf{X}^{k+1}, i\right) \quad (28)$$

where

$$\varpi^{k+1}\left(\mathbf{X}^{k+1}, i\right) = w_i^k f\left(\mathbf{X}^{k+1} \middle| \mathbf{X}_i^k\right) + u_i^k f\left(\mathbf{X}^{k+1} \middle| \mathbf{\Pi}\mathbf{X}_i^k\right) \quad (29)$$

and we have used the auxiliary variable i to denote an index in the mixture given by the prior, see (23), as in [12].

Let $\left(\tilde{\mathbf{X}}_i^{k+1}, j^i\right) \sim \upsilon(\cdot)$ and $\tilde{\mathbf{X}}_{i+N_{par}}^{k+1} = \mathbf{\Pi}\tilde{\mathbf{X}}_i^{k+1}$ for $i = 1, ..., N_{par}$ accounting for the fact that, according to (27), $q(\cdot)$ satisfies $q\left(\tilde{\mathbf{X}}_i^{k+1}, j^i\right) = q\left(\mathbf{\Pi}\tilde{\mathbf{X}}_i^{k+1}, j^i\right)$. Firstly, we should note that sampling and evaluating the weights for sequential importance sampling would be equivalent to this approach but using $j^i = i$. The weights of the particles are then

$$\tilde{w}_i^{k+1} \propto \frac{\ell\left(\mathbf{z}^{k+1} \middle| \tilde{\mathbf{X}}_i^{k+1}\right) \varpi^{k+1}\left(\tilde{\mathbf{X}}_i^{k+1}, j^i\right)}{q\left(\tilde{\mathbf{X}}_i^{k+1}, j^i\right)} \quad (30)$$

$$\tilde{u}_i^{k+1} \propto \frac{\ell\left(\mathbf{z}^{k+1} \middle| \tilde{\mathbf{X}}_i^{k+1}\right) \varpi^{k+1}\left(\mathbf{\Pi}\tilde{\mathbf{X}}_i^{k+1}, j^i\right)}{q\left(\tilde{\mathbf{X}}_i^{k+1}, j^i\right)} \quad (31)$$

To estimate α^{k+1}, see (20), we have to determine the particles that belong to A^{k+1} and which ones to $\bar{A}^{k+1}$ using (24). Therefore, for $i = 1, ..., N_{par}$, we let $\left(\mathbf{X}_i^{k+1}, \mathbf{X}_{i+N_{par}}^{k+1}, w_i^{k+1}, u_i^{k+1}\right) = \left(\tilde{\mathbf{X}}_i^{k+1}, \tilde{\mathbf{X}}_{i+N_{par}}^{k+1}, \tilde{w}_i^{k+1}, \tilde{u}_i^{k+1}\right)$ if $\tilde{\mathbf{X}}_i^{k+1} \in \bar{A}^{k+1}$ and $\left(\mathbf{X}_i^{k+1}, \mathbf{X}_{i+N_{par}}^{k+1}, w_i^{k+1}, u_i^{k+1}\right) = \left(\tilde{\mathbf{X}}_{i+N_{par}}^{k+1}, \tilde{\mathbf{X}}_i^{k+1}, \tilde{u}_i^{k+1}, \tilde{w}_i^{k+1}\right)$ otherwise. After this re-arrangement, it is known that $\varpi^{k+1}\left(\mathbf{X}_i^{k+1}\right) > \varpi^{k+1}\left(\mathbf{X}_{i+N_{par}}^{k+1}\right)$. However, this does not imply an inequality on the weights w_i^{k+1}, u_i^{k+1}, as they are based on $\varpi^{k+1}\left(\mathbf{X}^{k+1}, i\right)$ rather than $\varpi^{k+1}\left(\mathbf{X}^{k+1}\right)$. Therefore, there is no guarantee that $\alpha^{k+1} = 2\sum_{i=1}^{N_{par}} u_i^{k+1} < 1$, in fact, because of the normalisation

$$\sum_{i=1}^{N_{par}} \left(w_i^{k+1} + u_i^{k+1}\right) = 1 \quad (32)$$

α^{k+1} could reach the value 2 and this does not make sense.

We should note that conventional PFs have $O(N_{par})$ computational expense. However, to estimate α^{k+1}, we need to decide whether a sample belongs to A^{k+1} or $\bar{A}^{k+1}$. This process has a $O(N_{par}^2)$ computational complexity because of the evaluation of (24) and therefore, the overall computation expense is $O(N_{par}^2)$.

D. Marginal particle filter

To overcome the problem of the estimation of α^{k+1}, we use a marginal PF [13] in which the PF operates directly on the posterior pdf at the current time. In the marginal PF, samples are drawn in the same way as in conventional particle filtering but the weights are computed as

$$\tilde{w}_i^{k+1} \propto \frac{\ell\left(\mathbf{z}^{k+1} \middle| \tilde{\mathbf{X}}_i^{k+1}\right) \varpi^{k+1}\left(\tilde{\mathbf{X}}_i^{k+1}\right)}{q\left(\tilde{\mathbf{X}}_i^{k+1}\right)} \quad (33)$$

$$\tilde{u}_i^{k+1} \propto \frac{\ell\left(\mathbf{z}^{k+1} \middle| \tilde{\mathbf{X}}_i^{k+1}\right) \varpi^{k+1}\left(\mathbf{\Pi}\tilde{\mathbf{X}}_i^{k+1}\right)}{q\left(\tilde{\mathbf{X}}_i^{k+1}\right)} \quad (34)$$

where

$$q\left(\tilde{\mathbf{X}}_i^{k+1}\right) = \sum_{j=1}^{N_{par}} q\left(\tilde{\mathbf{X}}_i^{k+1}, j\right) \quad (35)$$

$\varpi^{k+1}(\cdot)$ is given by (23) and we have used (27). After the re-arrangement indicated in the Section IV-C, it is met that $w_i^{k+1} \geq u_i^{k+1}$. As shown in the Appendix, this implies that $\alpha^{k+1} \leq 1$ as required.

The exact implementation we use in the simulations in Section VI is the auxiliary marginal PF [13] in which the importance density for drawing normal particles is:

$$\upsilon\left(\mathbf{X}^{k+1}\right) \propto \sum_{i=1}^{N_{par}} \mu_i^{k+1}\left[w_i^k f\left(\mathbf{X}^{k+1} \middle| \mathbf{X}_i^k\right) + u_i^k f\left(\mathbf{X}^{k+1} \middle| \mathbf{\Pi}\mathbf{X}_i^k\right)\right] \quad (36)$$

where the so-called first-stage weights are

$$\mu_i^{k+1} \propto \ell\left(\mathbf{z}^{k+1} \middle| \hat{\mathbf{X}}_i^{k+1}\right)\left(w_i^k + u_i^k\right) \quad (37)$$

Table I: Auxiliary variable marginal PF with mirror particles

- For $i = 1 : N_{par}$
  - Calculate the first-stage weights μ_i^{k+1} using (37).
- Normalise μ_i^{k+1} to sum to one over $i = 1 : N_{par}$.
- For $i = 1 : N_{par}$
  - Draw a sample from $\upsilon(\cdot)$, given by (36):
    - Sample an index j from the distribution defined by μ_i^{k+1}.
    - Draw $\tilde{\mathbf{X}}_i^{k+1}$ from $f\left(\cdot \left| \mathbf{X}_j^{k+1} \right.\right)$ with probability $w_j^k / \left(w_j^k + u_j^k\right)$ or from $f\left(\cdot \left| \mathbf{\Pi X}_j^{k+1} \right.\right)$ with probability $u_j^k / \left(w_j^k + u_j^k\right)$.
  - Evaluate the weights of $\tilde{\mathbf{X}}_i^{k+1}$ and the mirror $\mathbf{\Pi}\tilde{\mathbf{X}}_i^{k+1}$, $\tilde{w}_i^{k+1}$ and $\tilde{u}_i^{k+1}$ using (33) and (34).
  - Rearrange the particles and weights to form $\mathbf{X}_i^{k+1}$, $\mathbf{\Pi X}_i^{k+1}$, w_i^{k+1} and u_i^{k+1} using (24).

and $\hat{\mathbf{X}}_i^{k+1}$ is the predicted state of particle i. The steps of the algorithm are shown in Table I. The drawback of the marginal PF in usual problems is that it has a $O(N_{par}^2)$ computational complexity. However, conventional PFs also have $O(N_{par}^2)$ computational complexity to estimate α^{k+1}. Therefore, marginal PFs do not add computational complexity to this problem.

V. Estimation using the decomposition

The aim is to estimate the target states without considering target labels as information about labelling is already given by α^k. After the targets move in close proximity for a long time, the MMSE estimator is not useful as it always provides estimates in the middle of the positions of the targets [4]. In this case, it is more advisable to use the MAP estimator [14]. Nonetheless, a suitable measure for analysing the performance of estimators of unlabelled targets is the OSPA metric [15]. Accordingly, the optimal estimator is the MMOSPA estimator [8] rather than the MAP or MMSE estimators. However, its computational expense is high as it requires a recursive algorithm.

The square OSPA distance between the sets X and $\hat{X}$ using the Euclidean metric without cut-off distance for two targets is [15]:

$$d_o^2\left(X, \hat{X}\right) = \frac{1}{2}\min\left[d^2\left(\mathbf{X}, \hat{\mathbf{X}}\right), d^2\left(\mathbf{\Pi X}, \hat{\mathbf{X}}\right)\right] \tag{38}$$

where $\mathbf{X}$ and $\hat{\mathbf{X}}$ are any ordered version of the sets X and $\hat{X}$ and, $d(\cdot,\cdot)$ is the Euclidean distance. The MMOSPA estimator is:

$$\hat{\mathbf{X}} = \int_{\mathcal{A}(\hat{\mathbf{X}})} \left[\mathbf{x}_1, \mathbf{x}_2\right]^T \pi^k\left(\left\{\mathbf{x}_1^k, \mathbf{x}_2^k\right\}\right) \mathrm{d}\mathbf{x}_1 \mathrm{d}\mathbf{x}_2 \tag{39}$$

where $\pi^k\left(\left\{\mathbf{x}_1^k, \mathbf{x}_2^k\right\}\right)$ is given by (9) and

$$\mathcal{A}\left(\hat{\mathbf{X}}\right) = \left\{\mathbf{X} : d^2\left(\mathbf{X}, \hat{\mathbf{X}}\right) = \min\left[d^2\left(\mathbf{X}, \hat{\mathbf{X}}\right), d^2\left(\mathbf{\Pi X}, \hat{\mathbf{X}}\right)\right]\right\} \tag{40}$$

The problem to calculate (39) is that the region of integration $\mathcal{A}\left(\hat{\mathbf{X}}\right)$ depends on the estimate $\hat{\mathbf{X}}$ and a recursive algorithm has to be used [8].

The PF representation of the form given by (21) directly allows the use of an estimator that produces lower OSPA errors than the MAP or MMSE estimators without increasing the computational burden as demonstrated with simulations in Section VI. The estimator exploits the knowledge of the regions A^k and $\overline{A}^k$ and its motivation is based on the Mahalanobis metric and a Gaussian approximation of the prior as explained in the following.

Let us use the Mahalanobis metric instead of the Euclidean metric in (38):

$$d_{om}^2\left(X, \hat{X}\right) = \frac{1}{2}\min\left[d_{m,\mathbf{S}}^2\left(\mathbf{X}, \hat{\mathbf{X}}\right), d_{m,\mathbf{S}}^2\left(\mathbf{\Pi X}, \hat{\mathbf{X}}\right)\right] \tag{41}$$

where

$$d_{m,\mathbf{S}}\left(\mathbf{X}, \hat{\mathbf{X}}\right) = \sqrt{\left(\mathbf{X} - \hat{\mathbf{X}}\right)\mathbf{S}^{-1}\left(\mathbf{X} - \hat{\mathbf{X}}\right)} \tag{42}$$

is the Mahalanobis distance between $\mathbf{X}$ and $\hat{\mathbf{X}}$ with covariance matrix $\mathbf{S}$. Then, we can define the Mahalanobis MMOSPA (MMMOSPA) estimator as

$$\hat{\mathbf{X}} = \int_{\mathcal{M}_{\mathbf{S}}(\hat{\mathbf{X}})} \left[\mathbf{x}_1, \mathbf{x}_2\right]^T \pi^k\left(\left\{\mathbf{x}_1^k, \mathbf{x}_2^k\right\}\right) \mathrm{d}\mathbf{x}_1 \mathrm{d}\mathbf{x}_2 \tag{43}$$

where

$$\mathcal{M}_{\mathbf{S}}\left(\hat{\mathbf{X}}\right) = \left\{\mathbf{X} : d_{m,\mathbf{S}}^2\left(\mathbf{X}, \hat{\mathbf{X}}\right) = \min\left[d_{m,\mathbf{S}}^2\left(\mathbf{X}, \hat{\mathbf{X}}\right), d_{m,\mathbf{S}}^2\left(\mathbf{\Pi X}, \hat{\mathbf{X}}\right)\right]\right\} \tag{44}$$

If we assume that the prior at time k, $\varpi^k\left(\mathbf{X}^k\right)$, is Gaussian with mean $\overline{\mathbf{X}}^k$ and covariance matrix $\mathbf{\Sigma}^k$, using (15) and (16), we get that

$$\overline{A}^k = \mathcal{M}_{\mathbf{\Sigma}^k}\left(\overline{\mathbf{X}}^k\right) \tag{45}$$

Therefore, we can define the "first-step" Gaussian MMMOSPA estimator $\hat{\mathbf{X}}_{om}$ as

$$\hat{\mathbf{X}}_{om} = \int_{\overline{A}^k} \left[\mathbf{x}_1, \mathbf{x}_2\right]^T \pi^k\left(\left\{\mathbf{x}_1^k, \mathbf{x}_2^k\right\}\right) \mathrm{d}\mathbf{x}_1 \mathrm{d}\mathbf{x}_2 \tag{46}$$

where we have called it "first-step" as it would be the first step of the recursion to calculate (43) starting at the predicted mean with covariance matrix $\mathbf{\Sigma}^k$. Using (9) and (21), the PF approximation of the first-step Gaussian MMMOSPA estimator is

$$\hat{\mathbf{X}}_{om} = \sum_{i=1}^{N_{par}} \left(w_i^k + u_i^k\right)\mathbf{X}_i^k \tag{47}$$

which is the posterior mean in $\overline{A}^k$ of the corresponding set pdf. The estimator (47) will be compared with MAP and MMSE estimators as regards OSPA state error in the next section.

VI. Simulations

We are going to analyse the label information and estimation performance of our algorithm in a scenario in which two targets are being tracked by a sensor network . The targets follow a nearly constant velocity model [16]:

$$p_d\left(\mathbf{x}_j^{k+1} \left| \mathbf{x}_j^k \right.\right) = \mathcal{N}\left(\mathbf{x}_j^{k+1}; \mathbf{F}\mathbf{x}_j^k, \mathbf{Q}\right) \tag{48}$$

Table II: Parameters of the simulation

Parameter	Value
SNR_0	30 dB
d_0	1 m
σ_u	1.8 $\mathrm{m/s^{3/2}}$
τ	0.5 s
N_{par}	10000

$$\mathbf{F} = \mathbf{I}_2 \otimes \begin{pmatrix} 1 & \tau \\ 0 & 1 \end{pmatrix} \tag{49}$$

$$\mathbf{Q} = \sigma_u^2 \mathbf{I}_2 \otimes \begin{pmatrix} \tau^3/3 & \tau^2/2 \\ \tau^2/2 & \tau \end{pmatrix} \tag{50}$$

where $j \in \{1, 2\}$, $\mathcal{N}(\mathbf{x}; \overline{\mathbf{x}}, \mathbf{Q})$ is the Gaussian pdf evaluated at $\mathbf{x}$ with mean $\overline{\mathbf{x}}$ and covariance matrix $\mathbf{Q}$, τ is the sampling period, and σ_u^2 is the continuous-time process noise intensity.

There is a grid of M sensors of side 10 m that forms a rectangle whose dimensions are 500 m $\times$ 700 m, i.e., there are 50 $\times$ 70 sensors and $M = 3500$. The measurement at time k is $\mathbf{z}^k = \left[z_1^k, z_2^k, ..., z_M^k\right]^T$ where z_r^k is the measurement taken by sensor r at time k and its equation for sensor r is:

$$z_r^k = h_r\left(\mathbf{X}^k\right) + \eta \tag{51}$$

where η is a zero-mean Gaussian noise with unit variance,

$$h_r\left(\mathbf{X}^k\right) = \sqrt{\sum_{j=1}^{2} SNR\left(d_{j,r,k}\right)} \tag{52}$$

$$SNR\left(d_{j,r,k}\right) = \begin{cases} SNR_0 & d_{j,r,k} \leq d_0 \\ \frac{SNR_0 d_0^2}{d_{j,r,k}^2} & d_{j,r,k} > d_0 \end{cases} \tag{53}$$

$$d_{j,r,k} = \sqrt{\left(x_j^k - m_{x,r}\right)^2 + \left(y_j^k - m_{y,r}\right)^2} \tag{54}$$

and $[m_{x,r}, m_{y,r}]^T$ are the coordinates of sensor r, SNR_0 is the maximum signal-to-noise ratio produced by a target and d_0 is the saturation distance. Equation (52) characterises the likelihood, see (4), and models the amplitude of the received acoustic signal at a sensor from incoherently emitting targets.

We use the parameters and the scenario, with 79 time steps, shown in Table II and Fig. 1, respectively. The trajectory of target one is fixed but we move the trajectory of target two depending on a parameter called d_x. When $d_x = 0$ m, both target states from time step 30 to 50 are exactly the same but they differ before time step 30 and after time step 50. Then, the distance in the x-axis that the trajectories are separated is d_x. Both target trajectories have been generated using the dynamic equation (48) fixing one part of the trajectory.

The prior pdf of the jth target at time step 0 is

$$\mathbf{x}_j^0 \backsim \mathcal{N}\left(\mathbf{p}_j^0; \overline{\mathbf{p}}_j^0, \sigma_{p0}^2 \mathbf{I}_2\right) \mathcal{N}\left(\mathbf{v}_j^0; \overline{\mathbf{v}}_j^0, \sigma_{v0}^2 \mathbf{I}_2\right) \tag{55}$$

where $\mathbf{p}_j^0$ and $\mathbf{v}_j^0$ are the position and velocity vector of target j at time 0, $\overline{\mathbf{p}}_j^0$ and $\overline{\mathbf{v}}_j^0$ are the expected position and velocity of target j at time 0 and, $\sigma_{p0}^2 \mathbf{I}_2$ and $\sigma_{v0}^2 \mathbf{I}_2$ are the covariance matrices of the position and velocity at time 0 . In each Monte Carlo run, $\overline{\mathbf{p}}_j^0$ is drawn from a Gaussian distribution whose mean is the real position of target j at time 0 and whose covariance matrix is $\sigma_{p0}^2 \mathbf{I}_2$ and $\overline{\mathbf{v}}_j^0$ is drawn from a Gaussian distribution whose mean is the real velocity of target j at time 0 and whose covariance matrix is $\sigma_{v0}^2 \mathbf{I}_2$. In the simulations, we use $\sigma_{0p} = 0.1\,\mathrm{m}$ and $\sigma_{v0} = 1\,\mathrm{m/s}$.

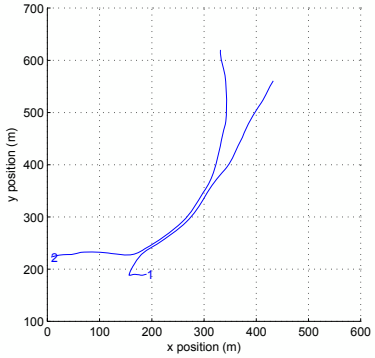

Figure 1: Scenario of the simulations for $d_x = 8\,\mathrm{m}$.

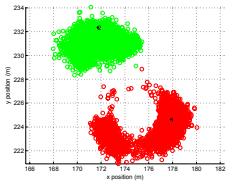

(a) $k = 26$ $\left(\alpha^{26} = 0\right)$

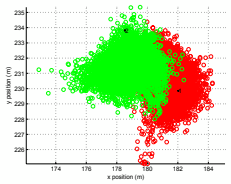

(b) $k = 27$ $\left(\alpha^{27} = 3.6 \cdot 10^{-129}\right)$

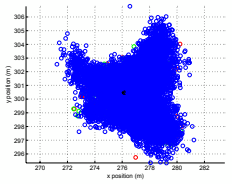

(c) $k = 41$ $\left(\alpha^{41} = 0.67\right)$

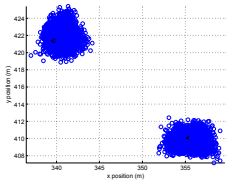

(d) $k = 57$ $\left(\alpha^{57} = 0.996\right)$

Figure 2: Constellations of particles at different time steps for $d_x = 0$ m and 5000 particles. For representation purposes, we assume a particle is labelled if $w_i^k > 3u_i^k$. Before the target crossing, particles are labelled. Red colour indicates the position of target 1 and green target 2. Finally, particles become blue that indicates that they have almost lost labelling information.

We show the constellations of particles at different time steps for an exemplar run in Fig. 2. Before the targets get close, the particles are labelled $w_i^k > u_i^k$. However, as they get in close proximity α^k increases and u_i^k increases. When $w_i^k \approx u_i^k$, the labels of the ith particle are lost as the particle $\mathbf{X}_i^k$ and $\mathbf{\Pi}\mathbf{X}_i^k$ are equally probable. After they separate, the estimated α^k reaches a steady value maintaining multimodality because our PF is designed to keep the information about target labelling after a crossing.

For different values of d_x, we carry out a Monte Carlo simulation with 50 realisations to obtain the averaged α^{79} (value of α^k at the end of the simulation) and the probability of successful labelling P_{sl}. As the value of α^k depends on the measurements, we use the same sequence of measurements for

Table III: Probability of successful labelling P_{sl} and α^{79} against the distance between targets

d_x(m)	Averaged α^{79}	P_{sl}
0	0.89	0.58
2	0.96	0.58
4	0.64	0.48
6	0.08	0.76
8	0.001	0.94
10	~ 0	1
12	0	1
14	0	1

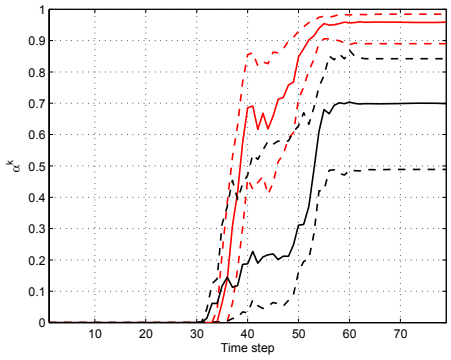

Figure 3: First, second and third quartiles of α^k plotted against time for $N_{par} = 10000$: In red colour: $d_x = 0\,\mathrm{m}$, in black colour: $d_x = 4\,\mathrm{m}$. For $d_x = 0\,\mathrm{m}$, α^k is close to one at the end as expected.

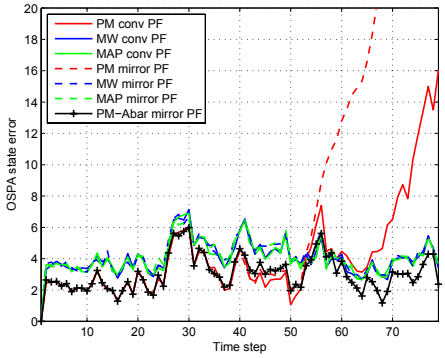

(a)

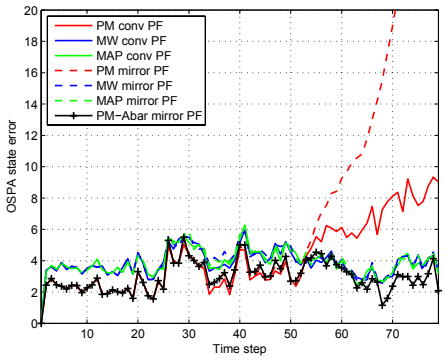

(b)

Figure 4: OSPA state error for a conventional auxiliary PF and the PF with mirror particles using MAP, the posterior mean (PM), the particle with maximum weight (MW) and the PM in $\overline{A}^k$: a) $d_x = 0$ b) $d_x = 4$. In the figure, Abar indicates $\overline{A}^k$. Averaged over all time steps, the posterior mean in $\overline{A}^k$ produces lower OSPA errors.

each d_x. The targets are successfully labelled if the permutation strictly variant part of the pdf has the right labelling at the final step of the simulation. In other words, we calculate the posterior mean and if it is closer to the targets with the right labelling than to the targets with the wrong labelling, the targets are properly labelled and they are not otherwise. The results are shown in Table III. For $d_x \geq 8\,\mathrm{m}$, α^{79} is very low and P_{sl} is very high. This indicates that for low values of α^{79}, one should be confident about the target labelling. On the contrary, for $d_x \leq 4\,\mathrm{m}$, α^{79} is over 0.5 and the probability of track swap is close to 0.5. Therefore, for these values of α^{79}, one cannot trust the labelling as it is practically at random. In general, it can be seen that as α^{79} gets lower, the probability of successful labelling roughly increases as expected.

We also show the value of first, second and third quartiles for α^k against time for $d_x = 0\,\mathrm{m}$ and $d_x = 4\,\mathrm{m}$ in Fig. 3. For $d_x = 0\,\mathrm{m}$, α^k is nearly one at the end. This means that the targets are not distinguishable as they have been a long time in close proximity. For $d_x = 4\,\mathrm{m}$, α^k reaches an intermediate value that indicates that there could be confusion in the target labels. In addition, the variance of the estimator of α^k is high as indicated by the quartiles.

We show the OSPA state error for a conventional auxiliary PF and the PF with mirror particles using the MAP [14], the posterior mean (PM), the estimator that the particle with maximum weight (MW) [17] and the PM in $\overline{A}^k$, see (47), in Fig. 4. It should be noted that using the MAP as proposed in [14] for a conventional PF increases its computational complexity to $O(N_{par}^2)$, the same of a marginal PF. For $d_x = 0\,\mathrm{m}$ and $d_x = 4\,\mathrm{m}$, one of the 50 realisations diverged for both PFs and the results shown are averaged over the convergent realisations. When the targets separate, the PM should lie somewhere in the middle of the real target states due to the multimodality of the posterior. This behaviour can be seen in the Fig. 4 as of time step 50 when the OSPA error of the PM for both filters increases considerably. The MAP and MW estimators do not have this property and are able to maintain lower errors after the targets separate. However, before the targets separate, their OSPA state errors are higher than the error of the PM and the PM in $\overline{A}^k$. By contrast, the PM in $\overline{A}^k$ achieves low OSPA state errors during the whole simulation. Additionally, it should be noted that before the targets get together, i.e., before time 30, the PM and the PM in $\overline{A}^k$ for both the conventional and mirror PFs produce the same error.

The OSPA state errors averaged over all time steps for the algorithms are shown in Table IV. In general, averaged over

Table IV: Averaged OSPA state error

d_x(m)	0	2	4	6
PM (conv PF)	4.30	4.93	4.22	2.66
MW (conv PF)	4.13	3.94	3.90	3.82
MAP (conv PF)	4.12	3.96	3.93	3.83
PM (mirror PF)	9.99	10.43	7.50	3.21
MW (mirror PF)	4.21	4.00	3.97	3.86
MAP (mirror PF)	4.17	4.00	3.98	3.87
PM in $\overline{A}^k$ (mirror PF)	3.07	2.96	3.02	2.74

all time steps, the PM in $\overline{A}^k$ achieves lower OSPA errors than the other estimators. In addition, its performance over the rest of the estimators gets better as d_x decreases.

VII. Conclusions

We have demonstrated that the information about target labels contained in the posterior can be used even if the measurements do not provide any information about target identity. To our knowledge, this algorithm has been the first approach to estimate recursively α^k in [4] to extract the information about target labelling. As such, we think it provides useful insight into the problem but at the expense of high computational burden. Nevertheless, it should be noted that even though the computational expense of our algorithm is $O(N_{par}^2)$, in principle, it can be sped up using the improved Gaussian transform or k-D trees [13], [18], [19].

We have also proposed an estimator that lowers the MOSPA error compared to other widely used estimators without increasing the computational burden of the algorithm.

A topic for future research is the generalisation of the unique decomposition of a pdf into variant and invariant parts for multiple targets as well as its implementation. Also, it should be noted that, in the generalisation for variable and unknown number of targets, the labels should explicitly be included in the state vector as done in [20].

VIII. Acknowledgements

Ángel F. García-Fernández is supported by an FPU Fellowship from Spanish MEC. This work was supported in part by the Spanish National Research and Development Program under Projects TEC2008-02148 and Comonsens (Consolider-Ingenio 2010, CSD2008-00010). Part of this work was done when Ángel F. García-Fernández was a visiting researcher at the University of Melbourne, Australia, in 2010.

The authors would like to thank Dr. Lennart Svensson for very valuable comments.

Appendix

In this Appendix, we show that if $w_i^k \geq u_i^k$ for $i = 1, ..., N_{par}$ then $\alpha^k \leq 1$. Summing over all the particles in $w_i^k \geq u_i^k$, we get

$$\sum_{i=1}^{N_{par}} w_i^k \geq \sum_{i=1}^{N_{par}} u_i^k \tag{56}$$

Then,

$$\sum_{i=1}^{N_{par}} w_i^k + \sum_{i=1}^{N_{par}} u_i^k \geq \sum_{i=1}^{N_{par}} u_i^k + \sum_{i=1}^{N_{par}} u_i^k \tag{57}$$

Using (22) and (32) in (57)

$$\alpha^k \leq 1 \tag{58}$$

References

[1] R. P. S. Mahler, *Statistical Multisource-Multitarget Information Fusion*. Artech House, 2007.

[2] M. R. Morelande, "Tracking multiple targets with a sensor network," in *9th International Conference on Information Fusion*, July 2006, pp. 1–7.

[3] J. Vermaak, S. J. Godsill, and P. Perez, "Monte Carlo filtering for multi target tracking and data association," *IEEE Transactions on Aerospace and Electronic Systems*, vol. 41, no. 1, pp. 309–332, Jan. 2005.

[4] H. Blom and E. Bloem, "Permutation invariance in Bayesian estimation of two targets that maneuver in and out formation flight," in *12th International Conference on Information Fusion*, July 2009, pp. 1296–1303.

[5] B. Ristic, S. Arulampalam, and N. Gordon, *Beyond the Kalman Filter: Particle Filters for Tracking Applications*. Artech House, 2004.

[6] Y. Boers and H. Driessen, "The mixed labeling problem in multi target particle filtering," in *10th International Conference on Information Fusion*, July 2007, pp. 1–7.

[7] Y. Boers, E. Sviestins, and H. Driessen, "Mixed labelling in multitarget particle filtering," *IEEE Transactions on Aerospace and Electronic Systems*, vol. 46, no. 2, pp. 792–802, April 2010.

[8] M. Guerriero, L. Svensson, D. Svensson, and P. Willett, "Shooting two birds with two bullets: How to find minimum mean OSPA estimates," in *13th Conference on Information Fusion*, July 2010, pp. 1–8.

[9] M. Arulampalam, S. Maskell, N. Gordon, and T. Clapp, "A tutorial on particle filters for online nonlinear/non-Gaussian Bayesian tracking," *IEEE Transactions on Signal Processing*, vol. 50, no. 2, pp. 174–188, Feb. 2002.

[10] J. Vermaak, A. Doucet, and P. Perez, "Maintaining multimodality through mixture tracking," in *Proceedings of the Ninth IEEE International Conference on Computer Vision, 2003*, vol. 2, Oct. 2003, pp. 1110–1116.

[11] G. Strang, *Introduction to linear algebra*. Wellesley - Cambridge Press, 2003.

[12] M. K. Pitt and N. Shephard, "Filtering via simulation: Auxiliary particle filters," *Journal of the American Statistical Association*, vol. 94, no. 446, pp. 590–599, Jun. 1999.

[13] M. Klaas, N. de Freitas, and A. Doucet, "Toward practical n^2 Monte Carlo: The marginal particle filter," in *Uncertainty in Artificial Intelligence*, 2005.

[14] H. Driessen and Y. Boers, "MAP estimation in particle filter tracking," in *IET Seminar on Target Tracking and Data Fusion: Algorithms and Applications*, April 2008, pp. 41–45.

[15] D. Schuhmacher, B.-T. Vo, and B.-N. Vo, "A consistent metric for performance evaluation of multi-object filters," *IEEE Transactions on Signal Processing*, vol. 56, no. 8, pp. 3447–3457, Aug. 2008.

[16] Y. Bar-Shalom, T. Kirubarajan, and X. R. Li, *Estimation with Applications to Tracking and Navigation*. John Wiley & Sons, Inc., 2002.

[17] J. Candy, "Bootstrap particle filtering," *IEEE Signal Processing Magazine*, vol. 24, no. 4, pp. 73–85, July 2007.

[18] R. Mittelman and E. Miller, "Nonlinear filtering using a new proposal distribution and the improved fast Gauss transform with tighter performance bounds," *IEEE Transactions on Signal Processing*, vol. 56, no. 12, pp. 5746–5757, Dec. 2008.

[19] C. Yang, R. Duraiswami, N. Gumerov, and L. Davis, "Improved fast Gauss transform and efficient kernel density estimation," in *Proceedings of the Ninth IEEE International Conference on Computer Vision*, Oct. 2003, pp. 664–671.

[20] A. F. García-Fernández and J. Grajal, "Multitarget tracking using the joint multitrack probability density," in *12th International Conference on Information Fusion*, July 2009, pp. 595–602.